Biocatalysis and Agricultural Biotechnology 8 (2016) 189–196

Contents lists available at ScienceDirect

Biocatalysis and Agricultural Biotechnology

journal homepage: www.elsevier.com/locate/bab

Antibacterial and antibiofilm assessment of *Momordica charantia* fruit extract coated silver nanoparticle

Balasubramanian Malaikozhundan [a], Baskaralingam Vaseeharan [a,*], Sekar Vijayakumar [a], Raja Sudhakaran [b], Narayanan Gobi [a], Ganesan Shanthini [c]

[a] *Biomaterials and Biotechnology in Animal Health Lab, Department of Animal Health and Management, Alagappa University, Karaikudi 630004, Tamil Nadu, India*

[b] *Aquaculture Biotechnology Laboratory, School of Bio-Sciences and Technology, VIT University, Vellore 632014, Tamil Nadu, India*

[c] *Department of Biotechnology, Vivekanandha College of Engineering for Women, Affiliated to Anna University, Tiruchengode 637205, Tamil Nadu, India*

ARTICLE INFO

Article history:
Received 27 June 2016
Accepted 8 September 2016
Available online 17 September 2016

Keywords:
Silver nanoparticle
Momordica charantia
Antibacterial
Antibiofilm
TEM

ABSTRACT

Silver nanoparticles were synthesized using the fruit extracts of *Momordica charantia* (*Mc*-AgNPs). The structural characterization of *Mc*-AgNPs was performed by UV–vis spectroscopy, X-ray diffraction (XRD), Fourier transform infrared spectroscopy (FTIR) and Transmission electron microscopy (TEM). UV–vis recorded the absorbance spectra at 460 nm. XRD shows the crystalline nature of silver nanoparticles with various Bragg's reflection peaks at 111, 200, 220 and 311. FTIR spectra of the synthesized *Mc*-AgNPs showed strong bands at 1382, 1203, 1151, 1102, 1013 and 654 cm^{-1} which corresponds to O–H, C–H, C–C, C–OH and C–N groups. TEM showed the spherical shape of *Mc*-AgNPs with particle size between 16 nm. The antibacterial activity of *Mc*-AgNPs was tested against Gram-positive and Gram-negative bacteria. *Mc*-AgNPs showed greater inhibition of *Enterococcus faecalis* at 100 $\mu g\ ml^{-1}$ compared to *Aeromonas hydrophila*. The biofilm inhibition of *Mc*-AgNPs was also higher against *E. faecalis* compared to *A. hydrophila*.

© 2016 Elsevier Ltd. All rights reserved.

1. Introduction

The problem of multiple drug resistance in microbes is growing and the outlook for the use of antimicrobial drugs in the future is still uncertain. Therefore, considerable attention is needed to reduce this problem, for example, to minimize the use of antibiotics, develop research to better understand the genetic mechanisms of resistance, and to continue studies to develop new drugs that are cost effective and eco-friendly. Therefore, the ultimate goal is to offer appropriate and efficient antimicrobial drugs to the society. Currently, nanotechnology has gained importance in the fields of biology, chemistry, physics, and material sciences (Elumalai et al., 2010; Singh et al., 2009). Nanotechnology has made it possible to develop and fabricate different dimensioned nanoparticles (Marambio-Jones and Hoek, 2010). The nanomaterials can be synthesized by different methods including chemical, physical, irradiation, and biological methods. The chemical or physical methods of nanoparticle synthesis have resulted in environmental contaminations, since the chemical procedures involved in the synthesis of nanomaterials generate a large amount of hazardous products (Zhang et al., 2008). Thus, there is a need for clean, safe, ecofriendly, and environmentally non-toxic method of nanoparticle synthesis. The green synthesis of nanoparticle using plant parts such as bark, root, leaves, fruit, flowers, rhizoids, and latex show different dimensions including the size, shape, and dispersion which have more efficacy than those synthesized from the chemical and physical procedures. Therefore, the use of plants for nanoparticle synthesis has compatibility for pharmaceutical and other biomedical applications, as they do not involve toxic chemicals for the synthesis of nanoparticles (Vijayaraghavan and Nalini, 2010; Crooks et al., 2001).

Among the several noble metal nanoparticles, silver nanoparticles (AgNPs) have attracted special attention due to their distinct properties, which include favorable electrical conductivity, chemical stability, catalytic and antibacterial activity (Sharma et al., 2009). Compared to larger AgNPs, smaller AgNPs have a greater binding surface and show more bactericidal activity (Kvitek et al., 2008). Their antimicrobial activities are attributed to the unique physico-chemical characteristics of AgNPs, such as the high surface area, mass ratio, high reactivity, and sizes in the nanometer range, which confer on them a major advantage for the development of alternative products against multi-drug resistant microorganisms (Martínez-Gutierrez et al., 2010).

Momordica charantia is a tropical and subtropical vine of the family Cucurbitaceae, widely grown in Asia, Africa, and the Caribbean for its edible fruit, which is extremely bitter. The Latin name *Momordica*

* Corresponding author.
E-mail address: vaseeharanb@alagappauniversity.ac.in (B. Vaseeharan).

http://dx.doi.org/10.1016/j.bcab.2016.09.007
1878-8181/© 2016 Elsevier Ltd. All rights reserved.

means "to bite," referring to the jagged edges of the leaves, which appear as if they have been bitten. It has shown antibacterial, anticancerous, antileukemic, antiprotozoal, antitumorous, antiviral, antiparasitic, antifungal, anti-obesity, anti-ulcer, hypoglycemi and, immune stimulant activities (Alam et al., 2009; Gupta et al., 2010; Agrawal and Beohar, 2010; Santos et al., 2012). It has been used by natural health practitioners for diabetes, cancer, high cholesterol, viral infections and bacterial infections (Grover and Yadav, 2004; Beloin et al., 2005). The main constituents of *M. charantia* responsible for the medicinal properties are triterpenes, proteins, steroids, alkaloids and other phenolic compounds (Budrat and Shotipruk, 2008; Saeed et al., 2010). Based on these perspectives, the present study was undertaken to synthesize silver nanoparticle using the fruit extract of *M. charantia*. In addition, the antibacterial and antibiofilm activity of the synthesized silver nanoparticle was tested against Gram positive and Gram negative bacteria.

2. Materials and methods

2.1. Collection of plant material

Momordica charantia was collected from the local vegetable market of Karaikudi, TamilNadu, India. The taxonomic identification of the plant was authenticated by the Botanical Survey of India, Coimbatore, TamilNadu, India. The voucher specimen numbered (DAHM-16-01) and preserved in the Department of Animal Health & Management, Alagappa University, Karaikudi.

2.2. Preparation of Momordica charantia extracts

Briefly, 10 g of fresh fruits of *M. charantia* was thoroughly washed 2–3 times with distilled water for surface cleaning, and surface sterilized with 0.1% $HgCl_2$ for 1 min to reduce microbial contamination (Singh et al., 2011). The sterile fruits were cut into fine pieces and boiled with 100 ml of double distilled water for 15 min at 60° C and filtered through Whatman number 1 filter paper and stored at 4 °C in the refrigerator for further experiments.

2.3. Synthesis of silver nanoparticles using the fruit extracts of M. momordica (Mc-AgNPs)

The fruit extract (1 ml) was added to 50 ml of 10^{-3} M $AgNO_3$ aqueous solution and kept at room temperature. The time of addition of extract into the aqueous $AgNO_3$ solution was considered as the start of the reaction. Under continuous stirring, after 10 min, the light yellow colour of $AgNO_3$ solution gradually changes to reddish brown colour indicates the formation of silver nanoparticles. The bioreduction of $AgNO_3$ ions in solution was monitored by periodic sampling of aliquots (0.1 ml) of aqueous component and measuring UV–vis spectra of the solution at different wavelengths (300–700 nm).

2.4. Characterization of Mc-AgNPs

2.4.1. UV–vis spectroscopic analysis

The optical properties of the silver nanoparticles (*Mc*-AgNPs) were studied using UV–visible absorption (UV-1700 Spectrometer of Shimadzu) spectrometer with samples in quartz cuvette. The absorption spectra of the synthesized *Mc*-AgNPs were monitored at different wavelengths ranged between 300 and 700 nm (Ankamwar et al., 2005).

2.4.2. X-ray diffraction (XRD) analysis

In order to determine the crystalline nature of nanoparticle, *Mc*-AgNPs were centrifuged, washed and air dried. The air dried powder was coated on the glass surface and then subjected to XRD analysis on a PAN analytical XRD analyzer (X'pert PRO) operating in transmission mode at 40 kV and 30 mA with Cu K radiation (Shankar et al., 2003). The grain size of the particles of the *Mc*-AgNPs was determined using Debye Sherrer's equation.

$$D = 0.94\lambda/B \cos\theta$$

2.4.3. Fourier transform infrared spectroscopy (FTIR) analysis

Two milligram of *Mc*-AgNPs was mixed with 200 mg of potassium bromide (FTIR grade) and pressed into a pellet. The sample pellet was placed into the sample holder and FTIR spectra were recorded in FTIR spectroscopy (Thermo Scientific Nicolet-iS5) at a resolution of 4 cm^{-1} (Chandran et al., 2006).

2.4.4. Transmission electron microscopy analysis

The size and surface morphology of *Mc*-AgNPs was determined following the method of Deepak et al. (2011). TEM analysis was performed by placing a small volume of *Mc*-AgNPs on carbon-coated copper grids and the solvent was allowed to evaporate for 30 min. TEM measurements were performed on JOEL model instrument 1200 EX instrument on carbon coated copper grids with an accelerating voltage of 80 kV.

2.5. Antibacterial assay

The agar well diffusion method (Perez et al., 1990) was used to screen the antibacterial activity of *Mc*-AgNPs against the pathogenic Gram positive (*Enterococcus faecalis* HQ693279) and Gram negative (*Aeromonas hydrophila* ATCC7966) bacteria. In vitro antimicrobial activity was screened by using Mueller Hinton Agar (MHA) obtained from Himedia (Mumbai). The MHA plates were prepared by pouring 15 ml of molten media into sterile petri plates. The plates were allowed to solidify for 5 min and 0.1% inoculum suspension of bacterial strains was swabbed uniformly and the inoculum was allowed to dry for 5 min. Then, wells were made on the plate using well puncher for loading the *Mc*-AgNPs. 50 μl of different concentration of *Mc*-AgNPs (25, 50, and 100 μg ml^{-1}) was loaded on the wells. The compound was allowed to diffuse for 5 min and the plates were kept for incubation at 37 °C for 24 h. The antibacterial efficacy of *Mc*-AgNPs was compared with $AgNO_3$ and fruit extract respectively. At the end of incubation, inhibition zones formed around the wells were measured with transparent ruler in millimeter.

2.6. Biofilm assay

Overnight culture of the Gram positive (*Enterococcus faecalis* HQ693279) and Gram negative (*Aeromonas hydrophila* ATCC7966) bacteria was diluted in the ratio of 1:100 in fresh TSB medium. Different concentrations of *Mc*-AgNPs (25, 50 and 100 μg ml^{-1}) were added to the 96-well microtiter plate and incubated at 37 °C for 48 h. Thereafter, the medium was removed and the wells were thoroughly washed with 1X PBS and 100 μl of 0.1% (w/v) crystal violet was added and incubated for 20 min. The crystal violet was removed and washed thoroughly with 1X PBS (Vijayakumar et al., 2015). For quantification of attached cells, the crystal violet was solubilized in absolute ethanol and the absorbance was measured at 570 nm. Reduction of the biofilm was correlated with the cells treated with *M. charantia* fruit extract alone (Data not shown).

2.7. In vitro biofilm inhibition assay

Glass slides (1 × 1 cm) were used to investigate the impact of *Mc*-AgNPs on the in vitro biofilm formation of bacterial strains. Briefly, bacterial biofilms were allowed to grow on glass slides

(1 × 1 cm) placed in 24-well polystyrene plates supplemented with *Mc*-AgNPs (25, 50 and 100 μg ml^{-1}) and incubated for 24 h at 37 °C. The glass slides were recovered and washed twice with 1X PBS before microscopy. Glass slides were then stained with crystal violet (0.4%) as before and examined using a Nikon inverted research microscope (ECLIPSE Ti 100) at 40 × magnification. Another set of glass slides with biofilms grown as above was washed with PBS, stained with acridine orange (0.1%) and the biofilm was quantified under a Confocal laser scanning microscopy (Carl Zeiss LSM 710) using 488 nm argon laser and BP 500–640 band pass emission filter. The running Zen 2009 software (Carl Zeiss, Germany) was also used to image the signal from glass samples (Vijayakumar et al., 2015).

2.8. Hydrophobicity index of bacterial biofilm

Overnight grown bacterial cells (control and nanoparticles treated) were resuspended in MHB, optical density at 595 nm was adjusted to 1.0 ± 0.01, and toluene (1 ml) was added to the cell suspension in a test tube and was vortexed for 1 min. The mixture was then allowed to settle for 30 min and the OD of the aqueous phase was measured. Hydrophobicity index (HI) of microbial cells was calculated by the formula

$$[(A0–A)A0–1] \times 100$$

where, A0 and A are the initial and final optical densities of the aqueous phase. The results were expressed as the proportion of the cells, which were excluded from the aqueous phase, determined using the above equation.

3. Results

3.1. Characterization of Mc-AgNPs

3.1.1. UV–visible spectroscopy

The addition of aqueous fruit extracts of *M. charantia* to 0.1 M solution of $AgNO_3$ at room temperature have led to the appearance of reddish brown colour indicating the formation of silver nanoparticles (*Mc*-AgNPs). *Mc*-AgNPs exhibits strong UV absorption spectra with the absorption peak at 460 nm due to its surface plasmon resonance (Fig. 1A).

3.1.2. X-ray diffraction (XRD) analysis

The XRD spectrum of *Mc*-AgNPs formed in the present experiment were in the form of nano crystals as evidenced by the Bragg's reflection peaks 2θ value at 38.42°, 44.36°, 64.40° and 77.49° which correspond to lattice planes at (111), (200), (220) and (311) have face centered cubic (FCC) crystal structure of AgNPs respectively (Fig. 1B). The average crystalline size of synthesized *Mc*-AgNPs is calculated by Scherrer equation and found to be 7.4 nm.

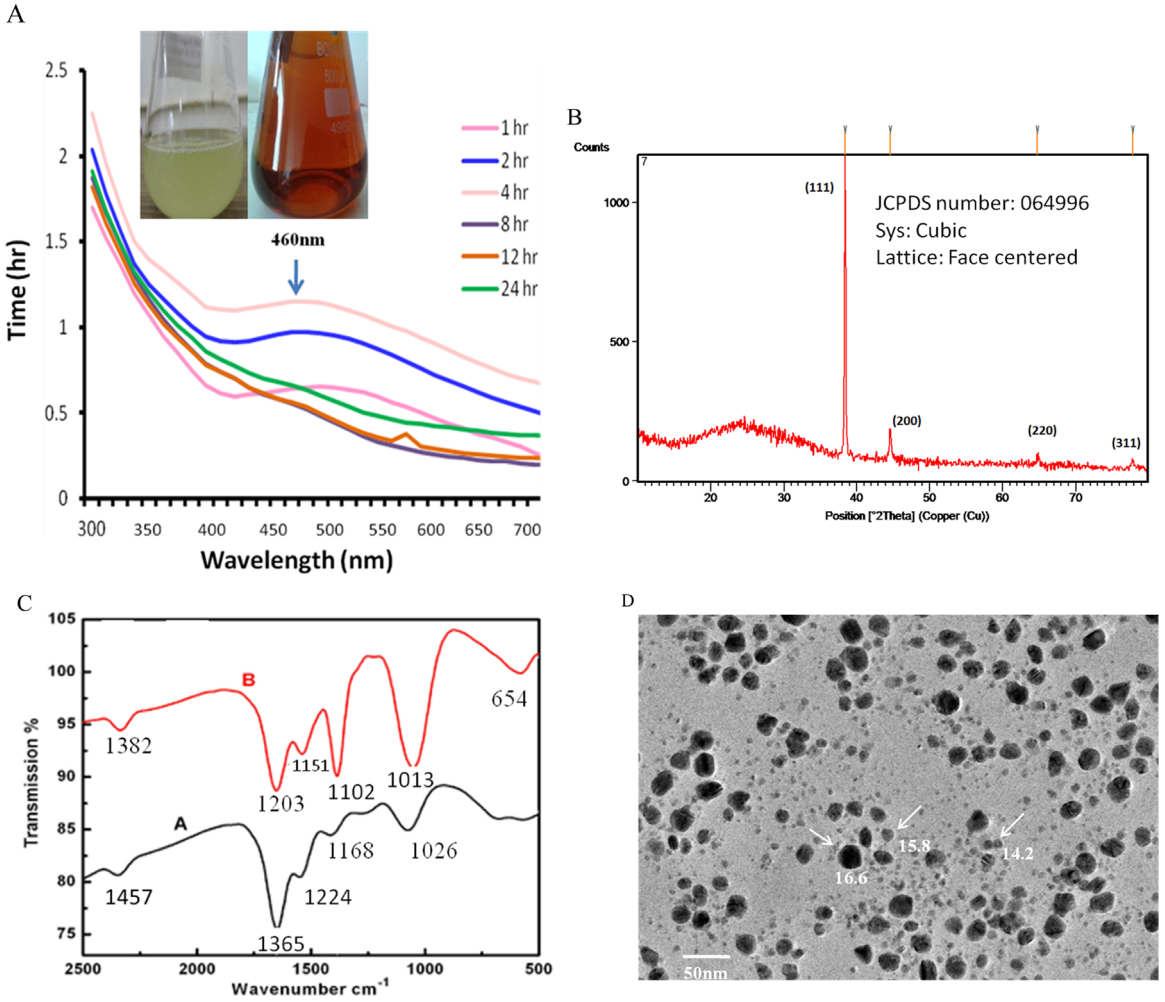


Fig. 1. A. UV–vis spectra of silver nanoparticles synthesized using *M. charantia* fruit extract at different reaction time. B. XRD spectra showing various Bragg's reflection peaks of silver nanoparticles synthesized using *M. charantia* fruit extract. C. FTIR spectra showing functional groups of silver nanoparticles synthesized using *M. charantia* fruit extract. D. TEM image of silver nanoparticles synthesized using *M. charantia* fruit extract.

3.1.3. Fourier transform infrared spectroscopy (FTIR) analysis

The interaction sites of *M. charantia* fruit extract and AgNPs were characterized by FTIR spectroscopy. The FTIR spectra of *Mc*-AgNPs in comparison with the fruit extract of *M. charantia* are shown in Fig. 1C. The FTIR spectra of the synthesized *Mc*-AgNPs showed functional groups at 1382, 1203, 1151, 1102, 1013 and 654 cm^{-1}. The intense broad band at 1382 cm^{-1} could be due to the stretching of O–H groups. The band observed at 1203 and 1151 cm^{-1} may be due to the stretching of C–H groups. The band at 1102 cm^{-1} corresponds to C–C stretching vibrations of aromatic amines. The band at 1013 cm^{-1} is characteristic of C–OH stretching of secondary alcohols. The band at 654 cm^{-1} region is characteristic of C–N stretching of aromatic phenols.

Table 1
Antimicrobial activity of $AgNO_3$, fruit extracts and *Mc*-Ag NPs against bacteria at 100 μg ml^{-1}.

Bacteria	Zone of inhibition (mm)*		
	Fruit extract (300 μg ml^{-1})	$AgNO_3$ (100 μg ml^{-1})	*Mc*-AgNPs
E. faecalis	10.2 ± 1.1	–	12.3 ± 1.2
A. hydrophila	7.4 ± 0.6	–	9.4 ± 1.4

* Values are mean ± SE of three replicates (significant at $P < 0.05$).

3.1.4. Transmission electron microscopy analysis

The size, structural morphology and crystallinity of biologically synthesized silver nanoparticles (*Mc*-AgNPs) are further confirmed by TEM micrograph images. The results revealed that *Mc*-AgNPs are spherical in shape and poly dispersed with no agglomeration. The average size of the *Mc*-AgNPs as revealed through TEM analysis is 16 nm (Fig. 1D).

3.2. Antibacterial assay

The antibacterial activity of *Mc* -AgNPs was investigated against Gram positive (*Enterococcus faecalis*) and Gram negative (*Aeromonas hydrophila*) bacteria by agar well diffusion method. The diameter of inhibition zones (mm) around each well loaded with *Mc*-AgNPs are represented in Table 1. The *Mc*-AgNPs synthesized using *M. charantia* fruit extracts are found to have greater antimicrobial activity against Gram-positive *E. faecalis* (12.3 mm) at 100 μg ml^{-1} (50 μl). The diameter of inhibition zone against Gram-negative *Aeromonas hydrophila* was 9.4 mm at 100 μg ml^{-1} (50 μl). On the otherhand, fruit extract of *M. charantia* showed inhibition zone of 10.2 mm and 7.4 mm against *E. faecalis* and *A. hydrophila* respectively at 300 μg ml^{-1}. The negative control (distilled water) (Figs. 2 and 3) and positive control ($AgNO_3$) (data not shown) showed no activity against none the bacterial strains (Table 2).

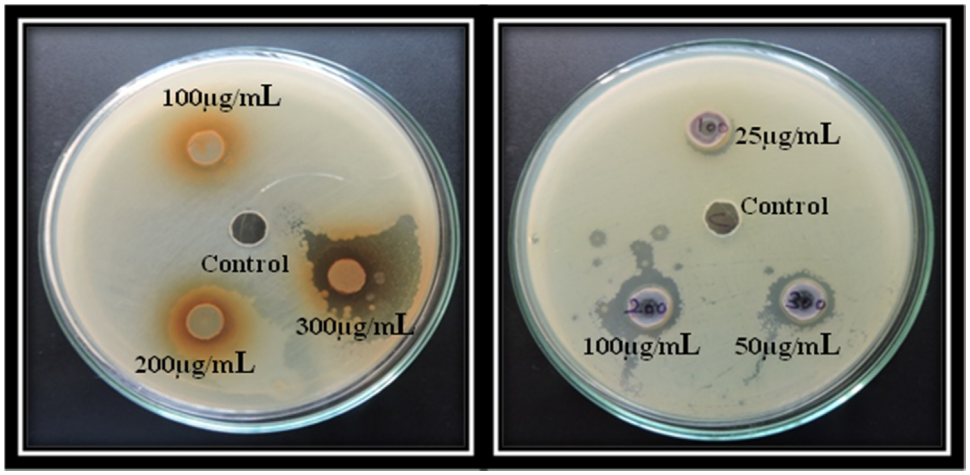


Fig. 2. Antibacterial activity against Gram-positive *E. faecalis* at different concentrations (μg ml^{-1}). (A) *M. charantia fruit extract* (B) *Mc*-AgNPs.

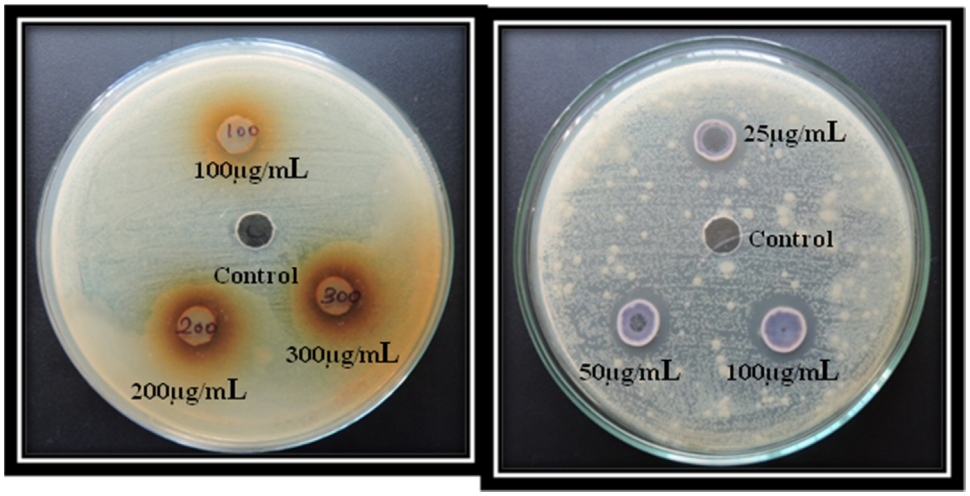


Fig. 3. Antibacterial activity against Gram-negative *A. hydrophila* at different concentrations (μg ml^{-1}). (A) *M. charantia fruit extract* (B) *Mc*-AgNPs.

Table 2
Minimum inhibitory concentrations of fruit extracts and *Mc*-Ag NPs against bacteria.

Bacteria	Minimum inhibitory concentration* ($\mu g\ ml^{-1}$)	
	Fruit extract	*Mc*-Ag NPs
E. faecalis	2.274 ± 0.2	1.965 ± 0.3
A. hydrophila	2.568 ± 0.8	2.012 ± 0.4

* Values are mean $\pm$ SE of three replicates (significant at $P < 0.05$).

3.3. Biofilm inhibition activity of Mc-AgNPs

The inhibition of biofilm formation of bacteria by *Mc*-AgNPs was assessed and visualized under light (Fig. 4) and confocal laser scanning microscopy (CLSM) (Figs. 5 and 6). *Mc*-AgNPs were found to significantly inhibit the biofilm formation of Gram-positive *E. faecalis* compared to that of Gram-negative *A. hydrophila*. Before treatment with *Mc*-AgNPs, the microscopic observation of the present study showed a well developed biofilm formation of bacterial strains. Treatment with *Mc*-AgNPs (100 $\mu g\ ml^{-1}$), the

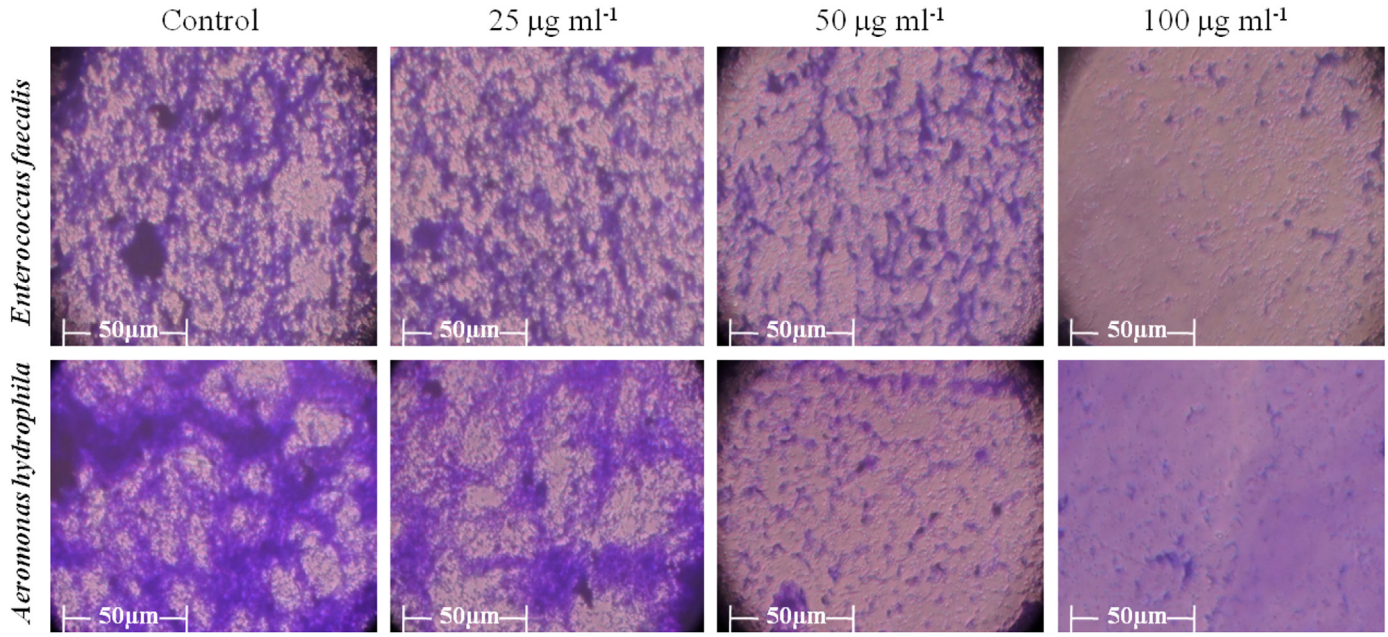


Fig. 4. Light microscopy images showing biofilm inhibition of *Mc*-AgNPs against *E. faecalis* and *A. hydrophila* at different concentrations.

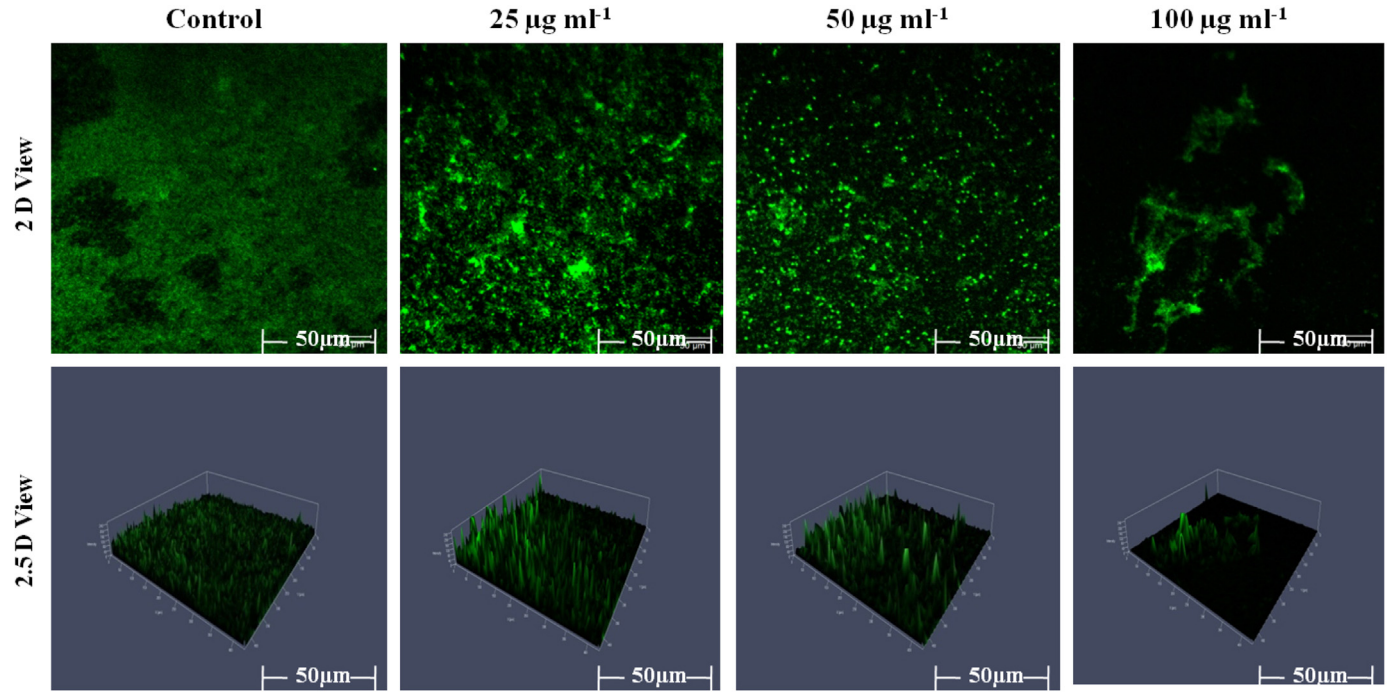


Fig. 5. Confocal laser scanning microscopy images showing biofilm inhibition of *Mc*-AgNPs against *E. faecalis* at different concentrations.

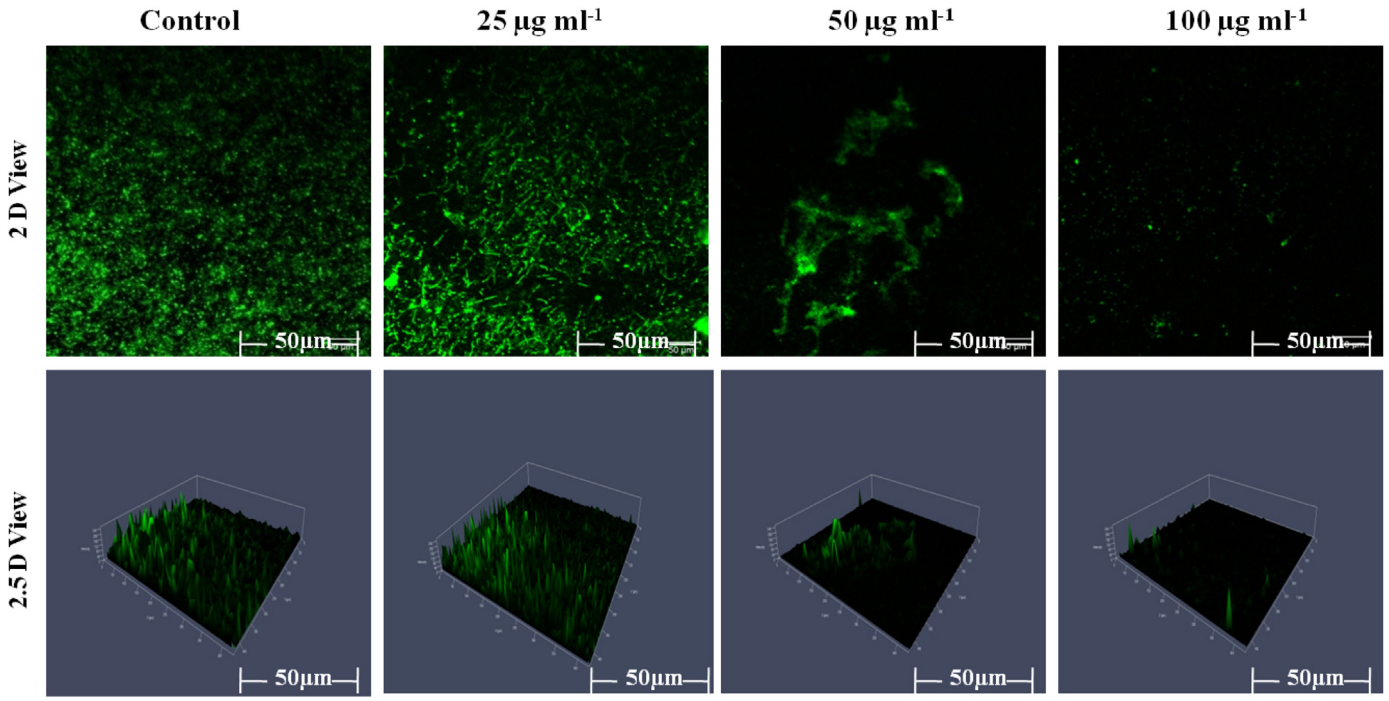


Fig. 6. Confocal laser scanning microscopy images showing biofilm inhibition of *Mc*-AgNPs against *A. hydrophila* at different concentrations.

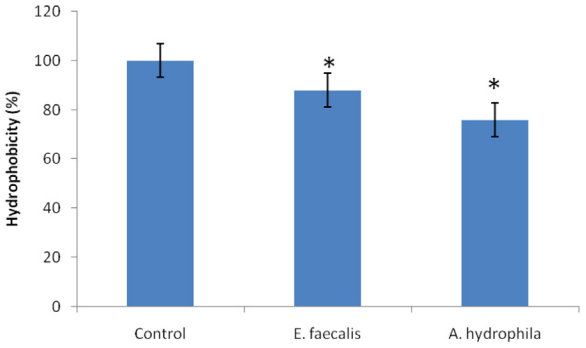


Fig. 7. Determination of hydrophobicity index of *E. faecalis* and *A. hydrophila* treated with 100 µg ml^{-1} of *Mc*-AgNPs for 24 h. Asterick indicates statistically significant values between treatments at $P \leq 0.05$ using ANOVA.

Gram-positive bacterium (*E. faecalis*) showed poor biofilm formation compared to that of the control sample. The inhibition of biofilm formation against Gram-negative bacterium (*A. hydrophila*) was comparatively lesser than that of Gram-positive bacterium. The percentage of hydrophobicity index was also decreased after treatment with *Mc*-AgNPs such that 88% and 76% hydrophobicity inhibition of *E. faecalis* and *A. hydrophila* respectively was observed as compared to untreated bacteria (Fig. 7)

4. Discussion

Silver (2003) stated that the first indication of silver nanoparticle (AgNPs) formation in a plant extract is visual; this is the appearance of a yellowish brown colour in an aqueous solution due to excitation of surface plasmon vibrations in silver nanoparticles. In the present study, we observed a reddish brown colloidal solution within the first few seconds of reaction of the silver nitrate solution with the aqueous fruit extract of *M. charantia*. Bindhu and Umadevi (2015) reported that the characteristic part of surface plasmon band of silver nanoparticles falls within the wavelength range of 350–500 nm. The same has been observed in the present study, where the appearance of surface plasmon peak around 460 nm confirms the formation of silver nanoparticles. These results are supported by Ajitha et al. (2015) who reported that the silver nanoparticle synthesized using the *M. charantia* leaf broth showed a distinct absorption at 424 nm.

The XRD spectra of *Mc*-AgNPs showed various Bragg's reflection peaks 2θ value at 38.42°, 44.36°, 64.40° and 77.49° which correspond to lattice planes at (111), (200), (220) and (311). This suggests that the synthesized *Mc*-AgNPs are face centered cubic crystals (FCC). The obtained data were matched with the Joint Committee on 250 Powder Diffraction Standards (JCPDS) file No. 04-0783. The broadening of Bragg's peaks indicates the formation of *Mc*-AgNPs and XRD patterns obtained in the present study are consistent with previous reports (Lokina et al., 2014; Ajitha et al., 2015).

FTIR measurement was carried out to identify the possible biomolecules responsible for capping and efficient stabilization of *Mc*-AgNPs. In the present study, the intense broad band at 1382 cm^{-1} could be due to the stretching vibrations of O–H groups. The band observed at 1203 and 1151 cm^{-1} may be due to the stretching of C–H groups. The band at 1102 cm^{-1} corresponds to C–C stretching vibrations of aromatic amines. The band at 1013 cm^{-1} is characteristic of C–OH stretching of secondary alcohols. The band at 654 cm^{-1} region is characteristic of C–N stretching of aromatic phenols. Presence of flavonoids, alkaloids, terpenoids, proteins, anthocyanins, sterols and carbohydrates in the *M. charantia* extract has been reported previously (Kumar et al., 2010; Leelaprakash et al., 2011; Annapoorani, 2013).

TEM analysis was performed to understand the topology and size of *Mc*-AgNPs. The TEM micrograph obtained in the present study showed polydispersed spherical nanoparticles with size between 16 nm. These results are in accordance with the findings of Ajitha et al. (2015) who reported that the size of silver nanoparticle synthesized from the *M. charantia* leaf extracts was 13 nm.

Silver is well known as one of the most universal antibacterial substances. Silver nanoparticles have been reported to show antibacterial activity against various pathogens (Yamanaka et al., 2005; Shahverdi et al., 2007; Yoon et al., 2007). The mechanism of

the bactericidal effect of silver colloid particles against bacteria is not very well-known. It is suggested that the antibacterial activity is probably derived, through the electrostatic attraction between negatively charged cell membrane of microorganism and positively charged nanoparticles. The inhibitory effect of silver on microorganisms tested is effected via two possible mechanisms First, is the electrostatic attraction between the negatively charged cell membrane of the microorganisms and the positively charged Ag, and second, is the formation of 'pits' in the cell wall of bacteria related to Ag concentration (Sondi et al., 2004). In the present study, among the tested bacteria, the maximum zone of inhibition (12.3 mm) was observed against *E. faecalis* followed by *A. hydrophila* (9.4 mm). The inhibition zone against Gram-negative bacteria was comparatively lesser than that of Gram-positive bacteria. The differences observed in the diameter of the zone of inhibition may be due to the difference in the susceptibility of different bacteria to the prepared silver nanoparticles (*Mc*-AgNPs). Bindhu and Umadevi (2015) reported that the differential sensitivity of Gram-positive and Gram-negative bacteria towards AgNPs possibly depends upon their cell structure, physiology, metabolism and their interaction with the charged silver nanoparticles. The effective interaction against Gram-positive bacteria was also due to absence of outer membrane in the cell wall. As a result of significant antibacterial activity, the synthesized *Mc*-AgNPs is effective in inhibiting the growth of both Gram-positive and Gram-negative bacteria.

At present, it becomes crucial to find alternative 'green' molecules or processes that are efficient in eradicating biofilm formation of bacteria in medical device and the environment. Mechanism of biofilm resistance to antimicrobial agents is the failure of an agent to penetrate the full depth of the biofilm (Weigel et al., 2007). In the present study, *Mc*-AgNPs were found to significantly inhibit the biofilm formation of *E. faecalis* and *A. hydrophila* at 100 $\mu g\ ml^{-1}$. It is suggested that NPs may directly diffuse through the exopolysaccharide layer through the pores and may impart anti-microbial function (Kalishwaralal et al., 2010). Exopolysaccharide and cell surface hydrophobicity play an important role in bacterium-host cell interactions and biofilm architectures in microbes. Borghi et al. (2011) previously reported that cell surface hydrophobicity helps in the reduction of biofilm production in different micro organisms including *Candida* sp. The present study also reports that treatment with *Mc*-AgNPs reduces the hydrophobicity index of both the Gram-positive and Gram-negative bacteria that leads to the inhibition of biofilm formation. In conclusion, the present study demonstrates the antibacterial and antibiofilm properties of *Mc*-AgNPs against Gram- positive and Gram-negative pathogenic bacteria.

5. Conclusion

Silver nanoparticle was easily synthesized using the fruit extract of *M. charantia* (*Mc*-Ag NPs). The synthesized *Mc*-Ag NPs showed enhanced antibacterial activity against Gram positive *E. faecalis* than Gram negative *A. hydrophila*. The antibiofilm activity was also greater against *E. faecalis* than *A. hydrophila*. *Mc*-Ag NPs reduced the biofilm growth of bacteria by decreasing their hydrophobicity index. This study concludes that *Mc*-Ag NPs could be effectively used in the control of pathogenic bacteria.

Conflict of interest

The authors do not have any conflicts of interest.

Acknowledgement

The author SV thank the Department of Science and Technology (DST) for grant of INSPIRE Fellowship (Ref. No: IF140145), New Delhi, India. Dr. B. Vaseeharan thank the Professor & Head, Department of Physics, Alagappa University for their help in XRD and FTIR analysis.

References

Agrawal, R.C., Beohar, T., 2010. Chemopreventive and anticarcinogenic effects of Momordica charantia extract. Asian Pac. J. Cancer Prev. 11, 371–375.
Ajitha, B., Reddy, Y.A.K., Reddy, P.S., 2015. Biosynthesis of silver nanoparticles using *Momordica charantia* leaf broth: evaluation of their innate antimicrobial and catalytic activities. J. Photochem. Photobiol. B 146, 1–9.
Alam, S., Asad, M., Asdaq, S.M.B., Prasad, V.S., 2009. Antiulcer activity of methanolic extract of *Momordica charantia* L. in rats. J. Ethnopharmacol. 123, 464–469.
Ankamwar, B., Chaudhary, M., Sastry, M., 2005. Synthesis and reactivity in inorganic. Metal-org. Nano-metal Chem. 35, 19–26.
Annapoorani, C.A., 2013. Screening of medicinal plant Momordica charantia leaf for secondary metabolites. Int. J. Pharm. Res. Dev. 5, 01–06.
Beloin, N., Gbeassor, M., Akpagana, K., Hudson, J., de Soussa, K., Koumaglo, K., Arnason, J.T., 2005. Ethnomedicinal uses of *Momordica charantia* (Cucurbitaceae) in Togo and relation to its phytochemistry and biological activity. J. Ethnopharmacol. 96, 49–55.
Bindhu, M.R., Umadevi, M., 2015. Antibacterial and catalytic activities of green synthesized silver nanoparticles. Spectrochim. Acta A Mol. Biomol. Spectrosc. 135, 373–378.
Borghi, E., Sciota, R., Biassoni, C., Cirasola, D., Cappelletti, L., Vizzini, L., et al., 2011. Cell surface hydrophobicity: a predictor of biofilm production in *Candida* isolates? J. Med Microbiol. 60, 689–690.
Budrat, P., Shotipruk, A., 2008. Extraction of phenolic compounds from fruits of bitter melon (*Momordica charantia*) with subcritical water extraction and antioxidant activities of these extracts. Chiang Mai J. Sci. 35 (1), 123–130.
Chandran, S.P., Chaudhary, M., Pasricha, R., Ahmad, A., Sastry, M., 2006. Synthesis of gold nanotriangles and silver nanoparticles using *Aloe vera* plant extract. Biotechnol. Prog. 22 (2), 577.
Crooks, R.M., Lemon, B.I., Sun, L., Yeung, L.K., Zhao, M., 2001. Dendrimer-encapsulated metals and semiconductors: synthesis, characterization, and applications. Top. Curr. Chem. 212, 82–135.
Deepak, V., Umamaheshwaran, P.S., Guhan, K., Nanthini, R.A., Krithiga, B., Hasika Jaithoon, N.M., Gurunathan, S., 2011. Synthesis of gold and silver nanoparticles using purified URAK. Colloids Surf. B 86, 353.
Elumalai, E.K., Prasad, T.N.V.K.V., Hema chandran, J., Therasa, S.V., Thirumalai, T., David, E., 2010. Extracellular synthesis of silver nanoparticles using leaves of *Euphorbia hirta* and their antibacterial activities. J. Pharmacol. Sci. Res. 2 (9), 549–554.
Grover, J.K., Yadav, S.P., 2004. Pharmacological actions and potential uses of *Momordica charantia*: a review. J. Ethnopharmacol. 93, 123–132.
Gupta, S., Raychaudhar, B., Banerjee, S., Mukhopadhyay, S., Datta, S.C., 2010. Momordicatin purified from fruits of *Momordica charantia* is effective to act as a potent antileishmania agent. Parasitol. Int. 59, 192–197.
Kalishwaralal, K., BarathManiKanth, S., Ram Kumar Pandian, S., Deepak, V., Gurunathan, S., 2010. Silver nanoparticles impede the biofilm formation by *Pseudomonas aeruginosa* and *Staphylococcus epidermidis*. Colloids Surf. B: Biointerface 79, 340–344.
Kumar, D.S., Sharathnath, K.V., Yogeshwaran, P., Harani, A., Sudhakar, K., Sudha, P., David, B., 2010. A medicinal potency of *Momordica charantia*. Int. J. Pharm. Sci. Res. 1, 95–100.
Kvitek, L., Panacek, A., Soukupova, J., Kolar, M., Vecerova, R., Prucek, R., Holecova, M., Zboril, R., 2008. Effect of surfactants and polymers on stability and antibacterial activity of silver nanoparticles (NPs). J. Phys. Chem. C 112, 5825–5834.
Leelaprakash, G., Rose, J.C., Gowtham, B.M., Krishna, J.P., Prasad, A.S., 2011. In vitro antimicrobial and antioxidant activity of *Momordica charantia* leaves. Pharmacophore 2, 244–252.
Lokina, S., Stephen, A., Kaviyarasan, V., Arulvasu, C., Narayanan, V., 2014. Cytotoxicity and antimicrobial activities of green synthesized silver nanoparticles. Eur. J. Med. Chem. 76, 256–263.
Marambio-Jones, C., Hoek, E.M.V., 2010. A review of the antibacterial effects of silver nanomaterials and potential implications for human health and the environment. J. Nanopart. Res. 12, 1531–1551.
Martinez-Gutierrez, F., Olive, P.L., Banuelos, A., Orrantia, E., Nino, N., Sanchez, E.M., Ruiz, F., Bach, H., 2010. Synthesis, characterization, and evaluation of antimicrobial and cytotoxic effect of silver and titanium nanoparticles. Nanomedicine 6 (5), 681–688.
Perez, C., Paul, M., Bazerque, P., 1990. An antibiotic assay by the agar well diffusion method. Acta Biol. Med. Exp. Exp. 15, 113.
Saeed, M., Shahzadi, I., Ahmad, I., Ahmad, R., Shahzad, K., Ashraf, M., Nisa, V., 2010. Nutritional analysis and antioxidant activity of bitter gourd (*Momordica charantia*) from Pakistan. Pharmacol. Online 1, 252–260.
Santos, K.K.A., Matias, E.F.F., Sobral-Souza, C.E., Tintino, S.R., Morais-Braga, M.F.B.,

et al., 2012. Trypanocide, cytotoxic and antifungal activities of *Momordica charantia*. Pharm. Biol. 50, 162–166.
Shahverdi, A.R., Fakhimi, A., Shahverdi, H.R., Minaian, S., 2007. Nanomed.: Nanotechnol. Biol. Med. 3, 168–171.
Shankar, S.S., Ahmad, A., Sastry, M., 2003. Geranium leaf assisted biosynthesis of silver nanoparticles. Biotechnol. Prog. 19, 1627–1631.
Sharma, V.K., Yngard, R.A., Lin, Y., 2009. Silver nanoparticles: green synthesis and their antimicrobial activities. Adv. Colloid Interface Sci. 145, 83–96.
Silver, S., 2003. Bacterial silver resistance: molecular biology and uses and misuses of silver compounds. FEMS Microbiol. Rev. 27, 341–353.
Singh, A.V., Patil, R., Kasture, M.B., Gade, W.N., Prasad, B.L.V., 2009. Synthesis of Ag-Pt alloy nanoparticles in aqueous bovine serum albumin foam and their cytocompatibility against human gingival fibroblasts. Colloids Surf. B 69 (2), 239–245.
Singh, V., Tyagi, A., Chauhan, P.K., Kumari, P., Kaushal, S., 2011. Int. J. Pharm. Pharm. Sci. 3 (4), 160–163.
Sondi, I., Salopek-sondi, B., 2004. Silver nanoparticles as antimicrobial agent: a case study on *E. coli* as a model for gram-negative bacteria. J. Colloid Interface Sci. 275, 177–182.
Vijayakumar, S., Vinoj, G., Malaikozhundan, B., Shanthi, S., Vaseeharan, B., 2015. *Plectranthus amboinicus* leaf extract mediated synthesis of zinc oxide nanoparticles and its control of methicillin resistant *Staphylococcus aureus* biofilm and blood sucking mosquito larvae. Spectrochim. Acta A Mol. Biomol. Spectrosc. 137 (25), 889–891.
Vijayraghavan, K., Nalini, S.P., 2010. Biotemplates in the green synthesis of silver nanoparticles. Biotechnol. J. 5, 1098–1110.
Weigel, L.W., Donlan, R.M., Shin, D.H., Jensen, B., Clark, N.C., McDougal, L.K., Zhu, W., Musser, A., Thompson, J., Kohlerschmidt, D., 2007. High-level vancomycin-resistant *Staphylococcus aureus* isolates associated with a polymicrobial biofilm. Antimicrob. Agents Chemother. 51, 231.
Yamanaka, M., Hara, K., Kudo, J., 2005. Bactericidal actions of a silver ion solution on *Escherichia coli*, studied by energy-filtering transmission electron microscopy and proteomic analysis. Appl. Environ. Microbiol. 71, 7589–7593.
Yoon, K., Byeon, J.H., Park, J., Hwang, J., 2007. Susceptibility constants of *Escherichia coli* and *Bacillus subtilis* to silver and copper nanoparticles. Sci. Total Environ. 373, 572–575.
Zhang, Y., Peng, H., Huang, W., Zhou, Y., Yan, D., 2008. Facile preparation and characterization of highly antimicrobial colloid Ag or Au nanoparticles. J. Colloid Interface Sci. 325, 371–376.